Supplemental material

Song et al., https://doi.org/10.1083/jcb.201711090

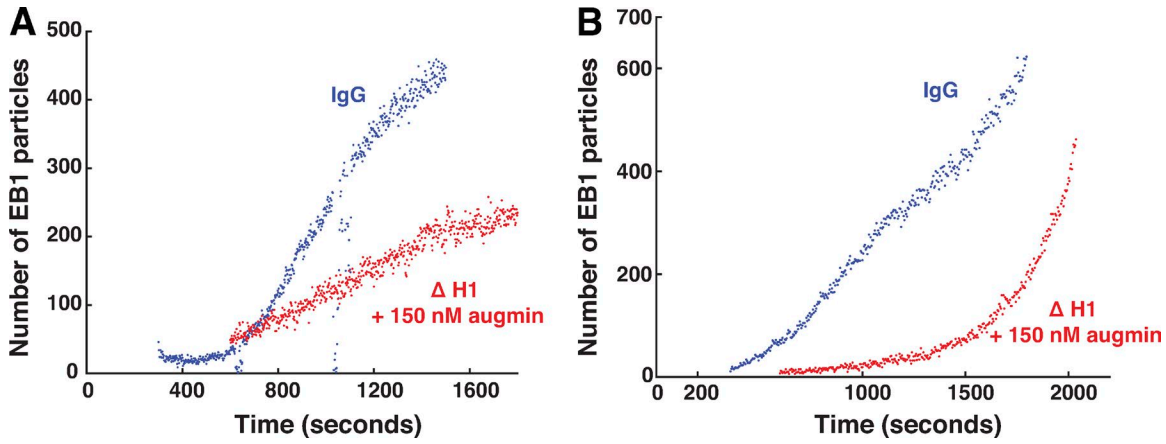

Figure S1. **Quantification of MT nucleation kinetics in IgG and augmin add-back conditions. (A and B)** We tracked and counted the number of EB1 comets, which each label a single MT and therefore represent the number of MTs. Five independent sets of experiments were performed, and two representative results are shown. See also Fig. 1 B.

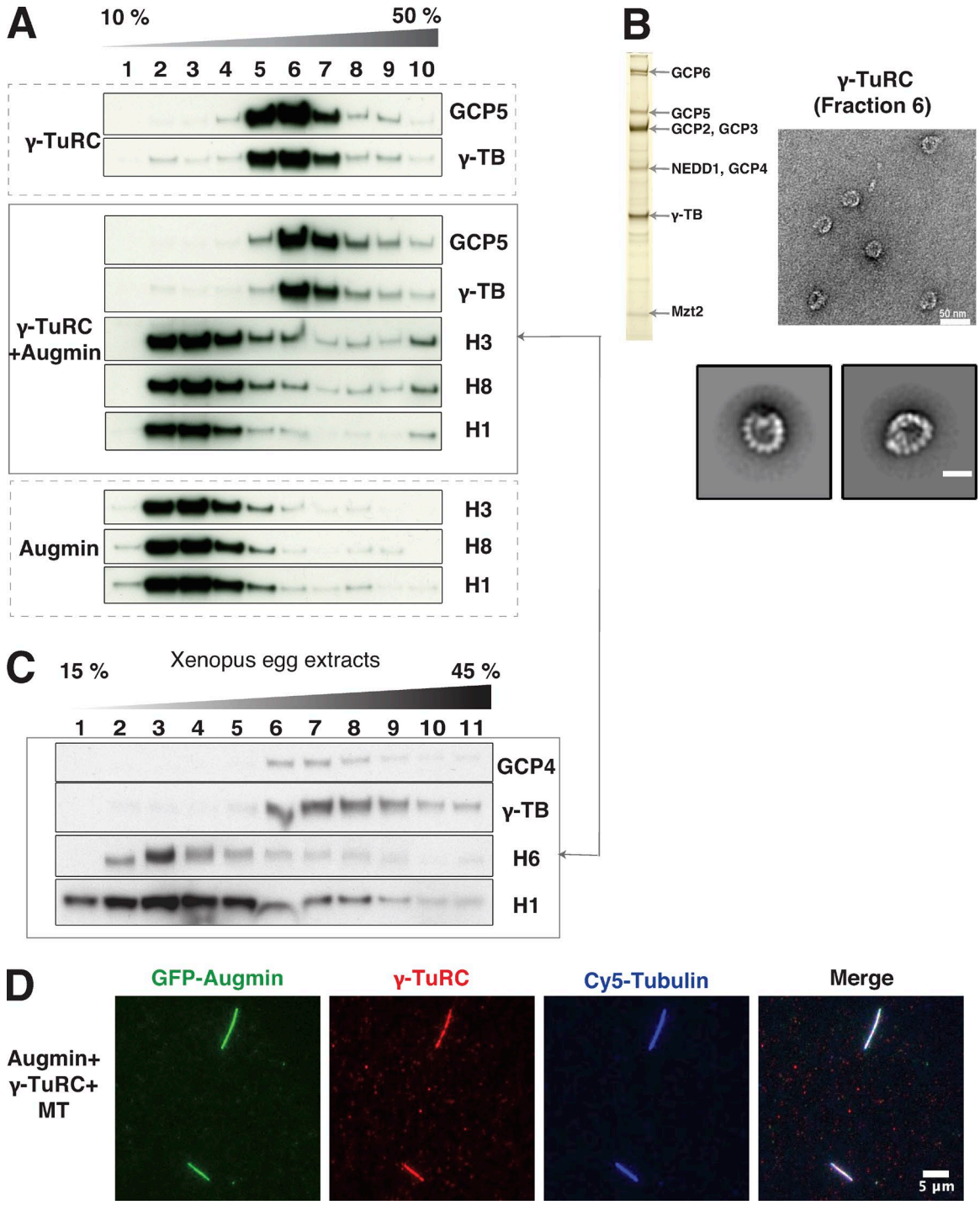

Figure S2. **Augmin binding to γ-TuRC in solution and when bound to microtubules. (A)** 100 nM augmin was mixed with 10 nM γ-TuRC, followed by sucrose gradient sedimentation (10–50% sucrose) to check the complex formation of augmin with γ-TuRC in vitro. Components of each complex were tracked by Western blot, showing that augmin has a peak at fraction 3 and γ-TuRC at fraction 6 (F6). Those peaks were not changed when mixed. **(B)** γ-TuRC samples from sucrose gradient sedimentation were analyzed by SDS-PAGE (silver staining; top left). γ-TuRC subunits were identified by mass spectrometry. Structure of γ-TuRC was analyzed by negative staining electron microscopy (92,000× magnification; top right). 2D class averages show a ring-shape structure of γ-TuRC (bottom). The reference-free 2D classification of the particle image stack was performed in Relion-2, using 20 classes and a regularization parameter T = 2. Bar, 20 nm. **(C)** The complex formation of endogenous augmin and γ-TuRC was analyzed by sucrose gradient centrifugation (15–45% sucrose) using *Xenopus* egg extracts, which is consistent with in vitro sucrose gradient profile of augmin and γ-TuRC mixture. Augmin (H6 and H1) and γ-TuRC (GCP4 and γ-TB) subunits were traced by Western blot. **(D)** Shown is an alternate field from the same IF sample exhibited in Fig. 2 D. Although Fig. 2 D shows the more common bundled MTs, shown here are single MTs (third panel) with augmin holocomplex (first panel) localizing γ-TuRC (middle panel). Single MTs were determined by signal intensity measurements matched to a control and augmin-mediated γ-TuRC localization to these single MTs.

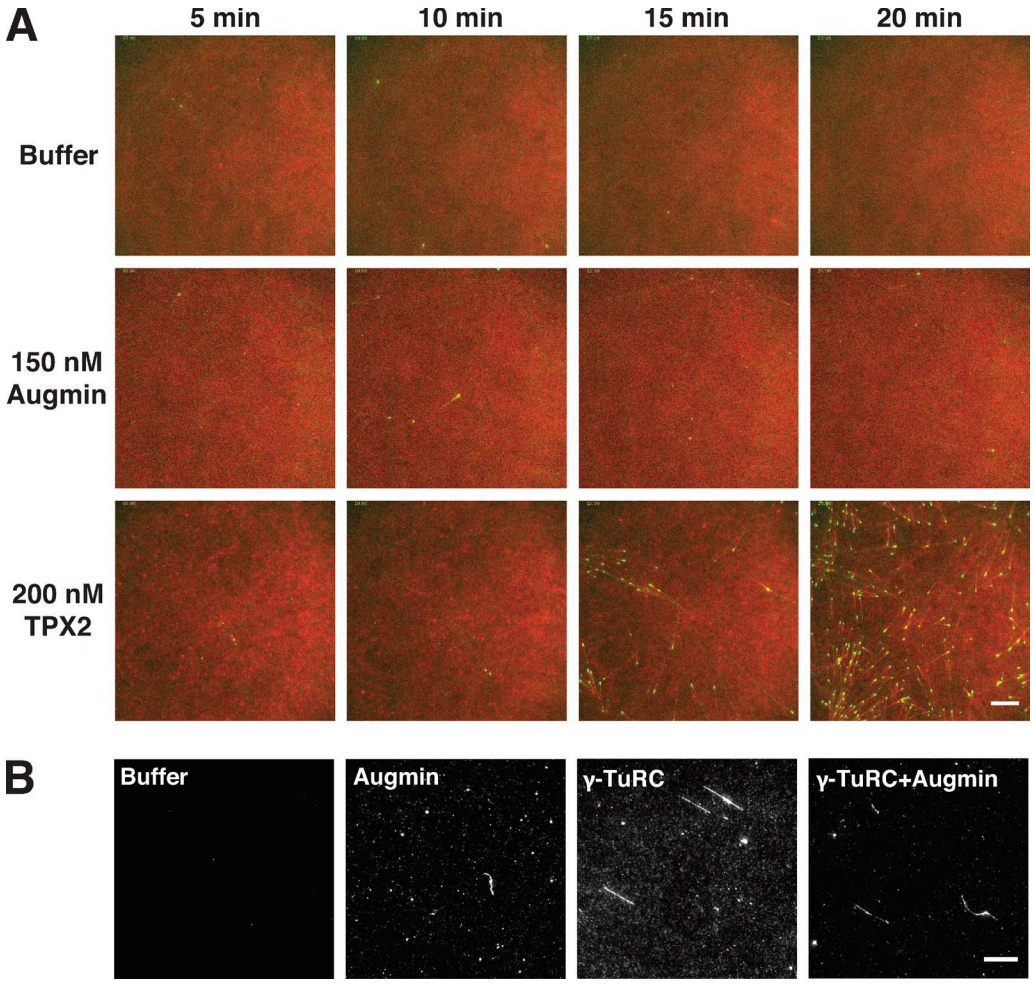

Figure S3. **Recobminant augmin does not enhance MT nucleation. (A)** Additions of 150 nM recombinant augmin or 200 nM TPX2 to *Xenopus* egg extracts in twofold excess of endogenous concentration. Addition of augmin does not induce MT nucleation in *Xenopus* egg extracts, in contrast to TPX2 (see 20-min time point). **(B)** MT nucleation assays with purified components. Purified γ-TuRC promotes MT nucleation of tubulin in the presence of GTP. However, 50 nM augmin alone does not nucleate MTs, nor does it activate γ-TuRC for MT nucleation in vitro. Bars, 10 µm.

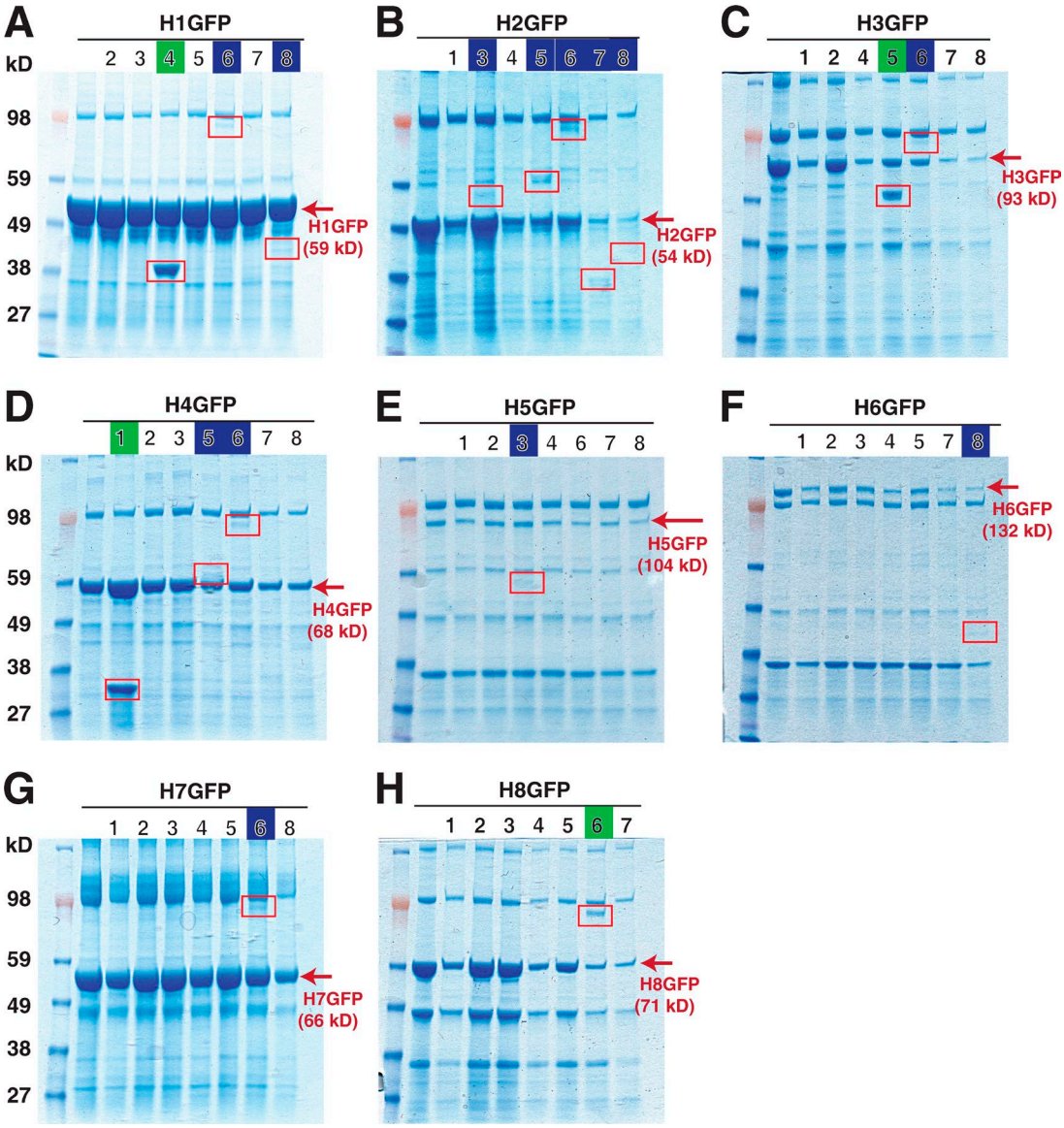

Figure S4. **In vitro pull-down assay results. (A)** N-terminal Strep-GFP–tagged H1 (H1GFP) was expressed alone and coexpressed with the other seven subunits. H1GFP is used as a bait of Strep-Tactin beads, and the other seven subunits are preys, showing H1GFP strongly interacts with H4 and weakly with H6 and H8. **(B)** H2GFP weakly interacts with H3, H5, H6, H7, and H8. **(C)** H3GFP strongly interacts with H5 and weakly with H6. **(D)** H4GFP strongly interacts with H1 and weakly with H5 and H6. **(E)** H5GFP weakly interacts with H3. **(F)** H6GFP weakly interacts with H8. **(G)** H7GFP weakly interacts with H6. **(H)** H8GFP strongly interacts with H6.

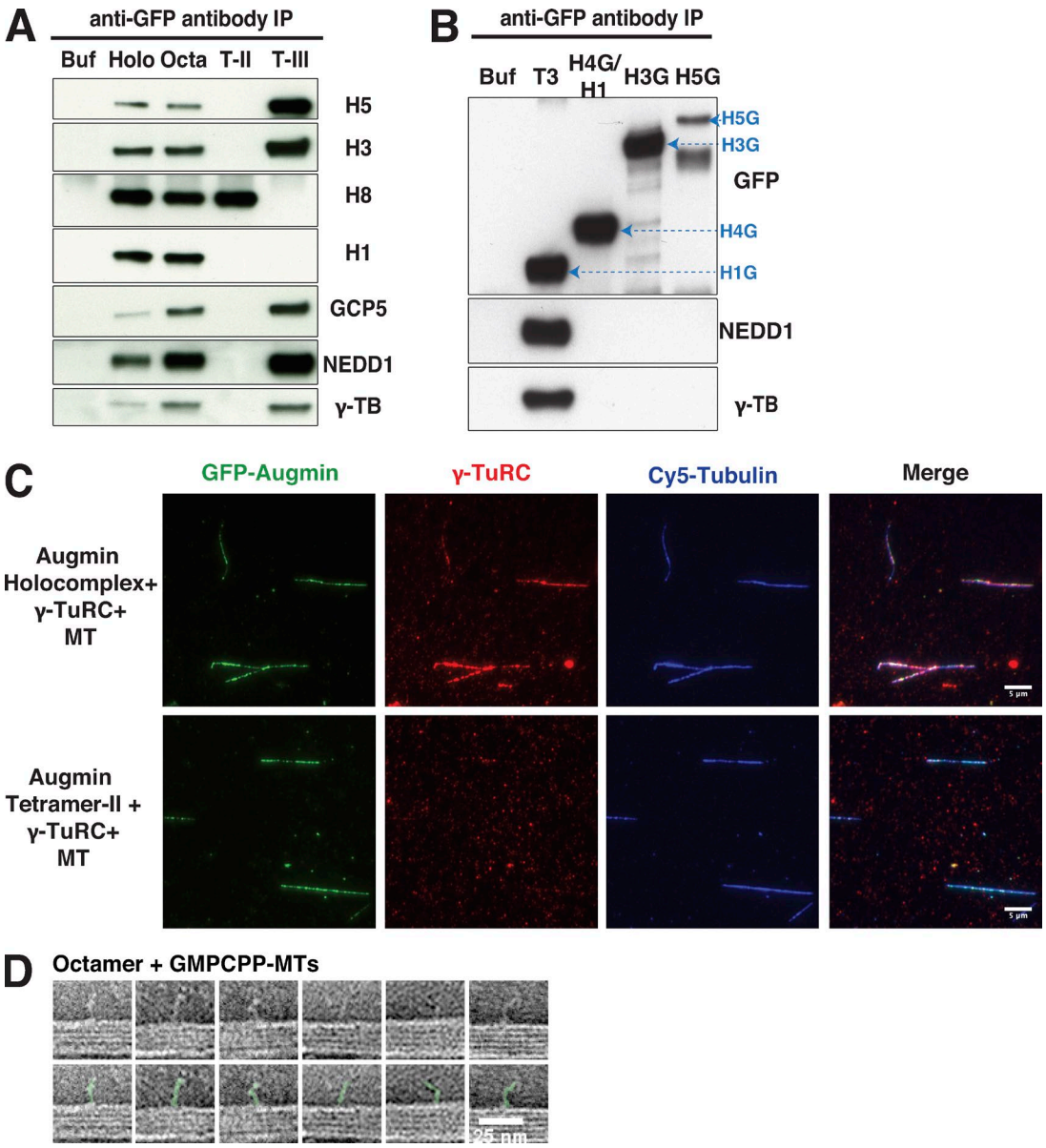

Figure S5. **Analysis of how augmin interacts with γ-TuRC and MTs. (A)** IP was performed to examine whether recombinant augmin complexes interact with endogenous γ-TuRC after augmin add back to the ID extract. Anti-GFP antibody was used for IP because it binds only to the recombinant augmin and is common among the four complexes. Augmin and γ-TuRC subunits were detected by Western blot. **(B)** γ-TuRC interactions of T-III components (H4GFP/H1 dimer, H3GFP, and H5GFP) were examined by IP using αGFP in extracts. **(C)** IF data demonstrate that augmin holocomplex, but not T-I, mediates localization of γ-TuRC to MTs. Data presentation and acquisition match IF data in Fig. 2 D. **(D)** Representative images of augmin octamer on GMPCPP-MTs. Bar, 20 nm.

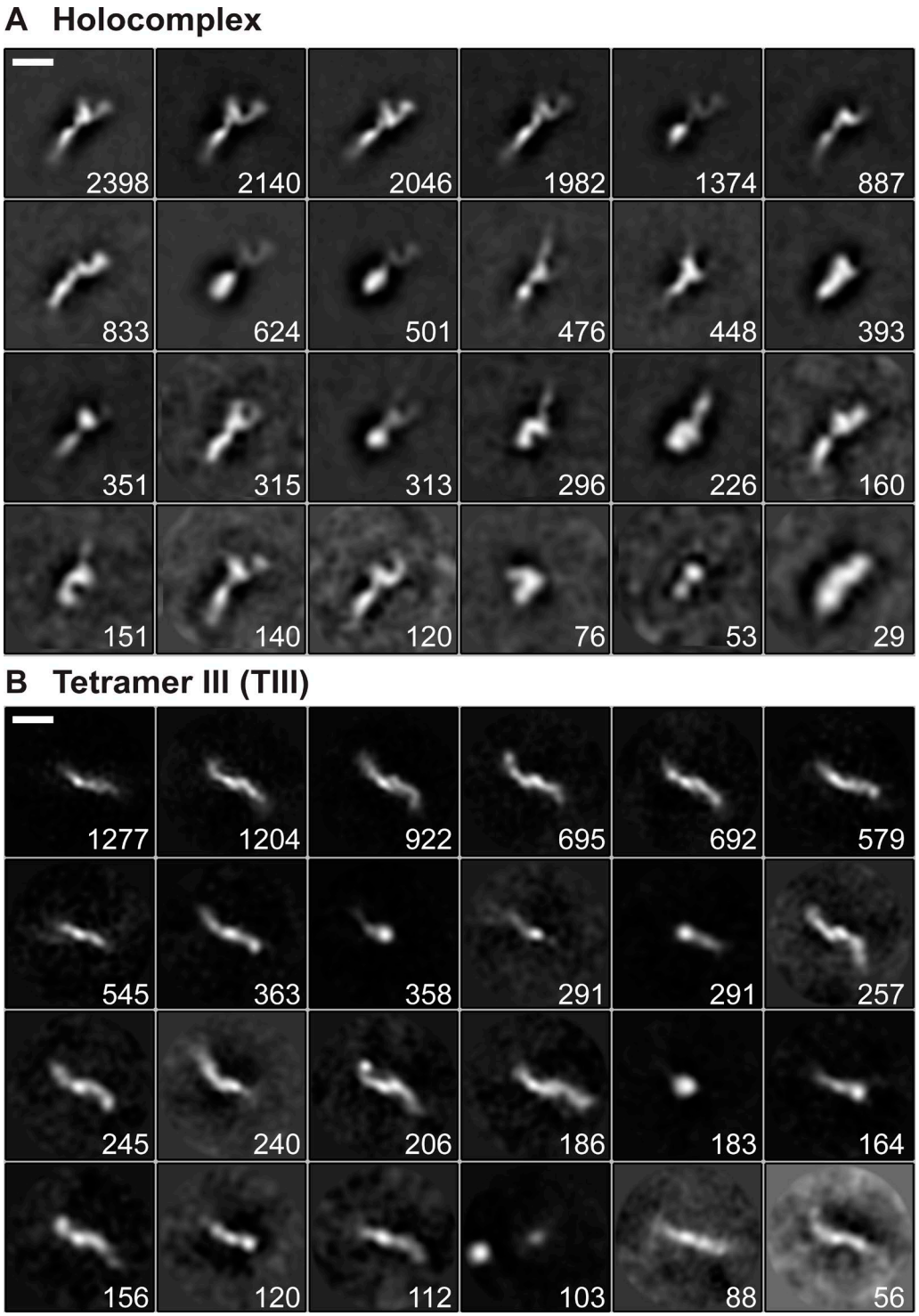

Figure S6. **Negative-stain analysis of augmin.** Reference free 2D class averages of augmin complexes generated by Relion-2. **(A and B)** For both augmin holocomplex (A) and T-III (B), the top 24 representative class averages with the most number of particles (as indicated at the lower right corner of each image) are shown. Bars, 20 nm.

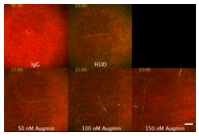

Video 1. **Recombinant augmin is active and can replace endogenous augmin.** Recombinant augmin is added back to immunodepleted extracts, showing recovering branching MT nucleation activity in a concentration-dependent manner. Images were collected using TIRF microscopy at 2-s intervals. mCherry-EB1 is pseudocolored in green, and Cy5-tubulin is shown in red. The movie was generated at 40 frames per second. Time is shown in the format of minutes:seconds. Bar, 10 µm. The video corresponds to Fig. 1 B.

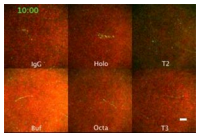

Video 2. **Augmin complexes have varying activites.** Augmin complexes depicted were added to immunodepleted extracts. IgG indicates *Xenopus* egg extracts without ID of augmin (ID using IgG antibody), and Buf means ID of extracts with CSF-XB buffer addition. Images were collected using TIRF microscopy at 2-s intervals. mCherry-EB1 is pseudocolored in green, and Cy5-tubulin is shown in red. The movie was generated at 40 frames per second. Time is shown in the format of minutes:seconds. Bar, 10 µm. The video corresponds to Fig. 4 C.